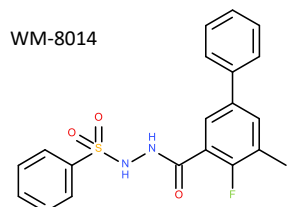


Supplemental Material to DMD/2020/090563

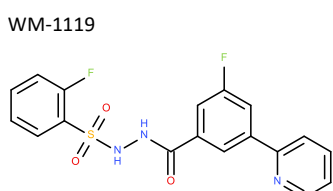
Concentration dependency of the unbound partition coefficient $K_{p_{uu}}$ and its application to correct for exposure related discrepancies between biochemical and cellular potency of KAT6A inhibitors
Trünkle C., Lechner C., Korr D., Bouché L., Barak N., Fernández-Montalván A., Süssmuth R.D. and Reichel A.

Drug Metabolism and Disposition

A



B

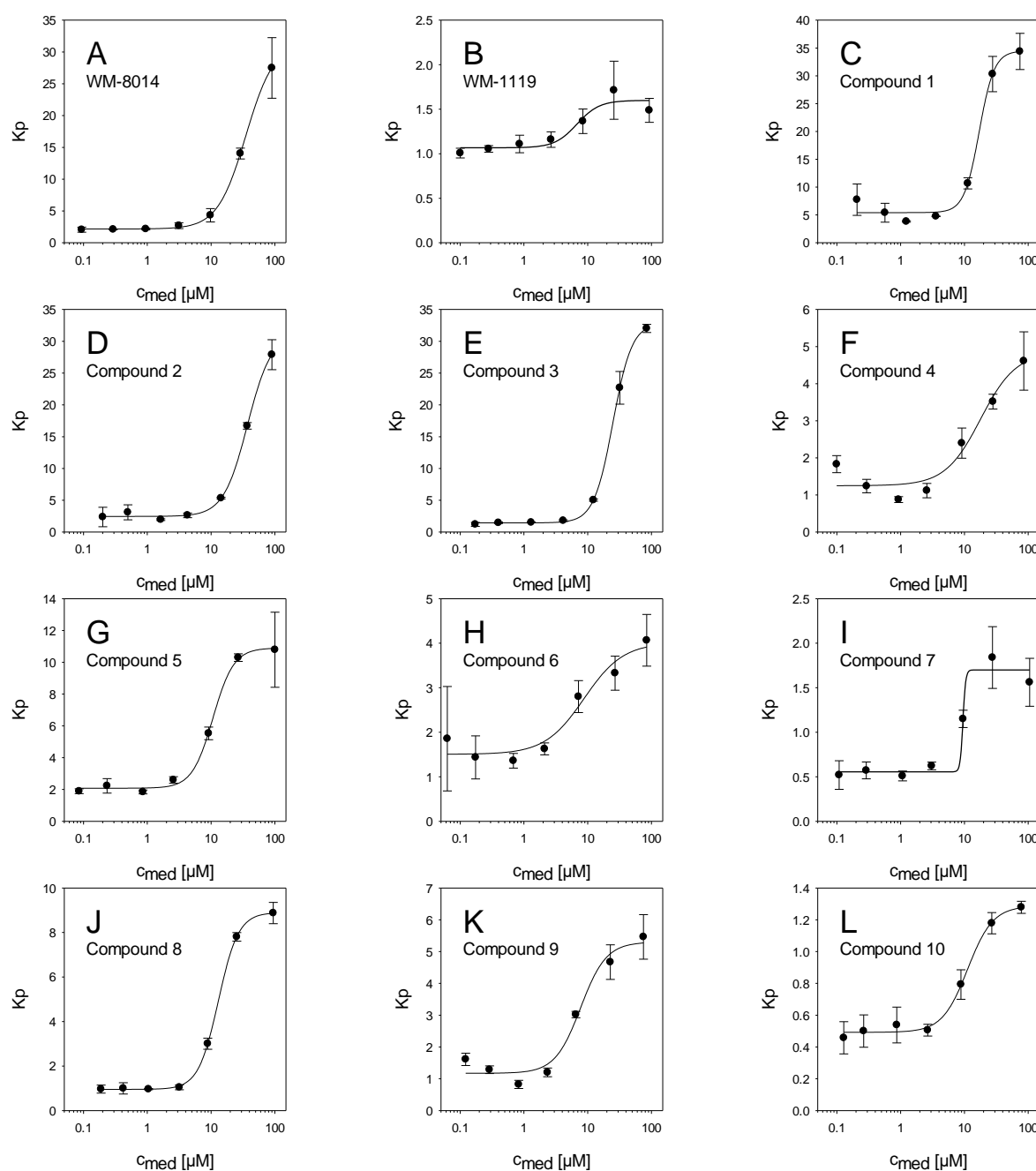


Supplemental Figure 1: Chemical structure of previously published KAT6A inhibitors WM-8014 (A) and WM-1119 (B) that were included in this study.

Supplemental Material to DMD/2020/090563

Concentration dependency of the unbound partition coefficient $K_{p,uu}$ and its application to correct for exposure related discrepancies between biochemical and cellular potency of KAT6A inhibitors
 Trünkle C., Lechner C., Korr D., Bouché L., Barak N., Fernández-Montalván A., Süssmuth R.D. and Reichel A.

Drug Metabolism and Disposition

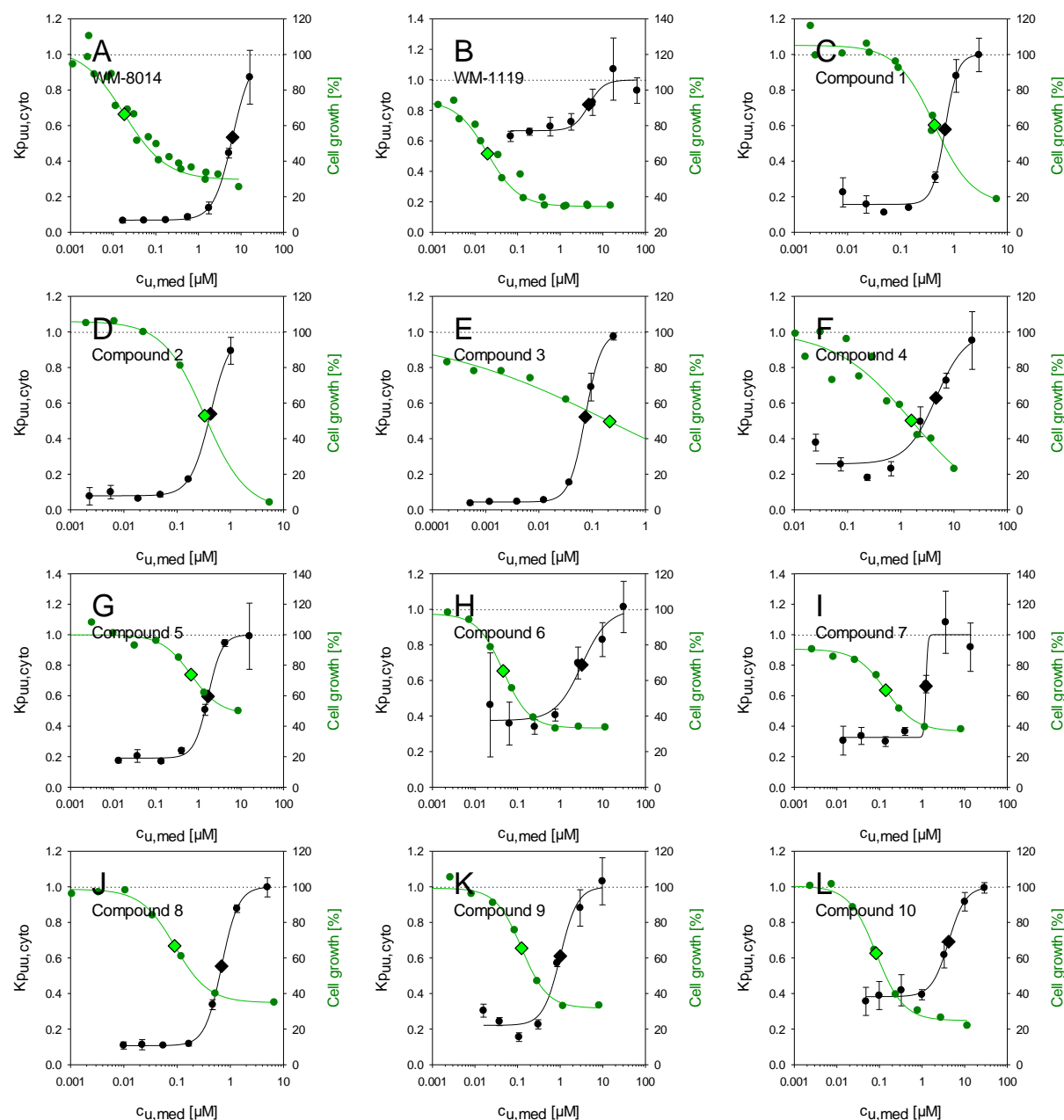


Supplemental Figure 2: Concentration dependent cellular accumulation ratio (K_p) in ZR75-1 cells for all investigated KAT6A inhibitors in this study (A-L). The line represents curve fitting of Eq. 3 to the data points to estimate $K_{p,sat}$ and $K_{m,app}$. The accuracy of $f_{u,cyto}$ estimates depends on how reliable $K_{p,sat}$ can be estimated.

Supplemental Material to DMD/2020/090563

Concentration dependency of the unbound partition coefficient $K_{P_{uu}}$ and its application to correct for exposure related discrepancies between biochemical and cellular potency of KAT6A inhibitors
 Trünkle C., Lechner C., Korr D., Bouché L., Barak N., Fernández-Montalván A., Süßmuth R.D. and Reichel A.

Drug Metabolism and Disposition



Supplemental Figure 3: Concentration dependent $K_{P_{uu,cyto}}$ determined with the saturation method and observed *in vitro* potency against ZR75-1 cells for all KAT6A inhibitors in this study (A-L).

Supplemental Material to DMD/2020/090563

Concentration dependency of the unbound partition coefficient $K_{p_{uu}}$ and its application to correct for exposure related discrepancies between biochemical and cellular potency of KAT6A inhibitors
 Trünkle C., Lechner C., Korr D., Bouché L., Barak N., Fernández-Montalván A., Süssmuth R.D. and Reichel A.

Drug Metabolism and Disposition

Supplemental Table 1: *In silico* physicochemical compound properties of KAT6A inhibitors calculated by ADMET PredictorTM and *in vitro* Caco-2 permeability.

Compound	<i>In silico</i> prediction of physicochemical properties			Caco-2 P_{app} [nm/s] ^a
	$\log D_{pH7.5}$	acidic pK_a	Predominant charge state at pH = 7.4	
WM-8014	2.9	8.8	neutral	260
WM-1119	1.9	7.7	neutral	197
Compound 1	4.5	7.6	neutral	n.d.
Compound 2	2.8	3.6	negative	55
Compound 3	3.1	3.6	negative	96
Compound 4	2.3	4.1	negative	67
Compound 5	2.7	3.8	negative	95
Compound 6	2.4	4.3	negative	146
Compound 7	1.9	4.1	negative	53
Compound 8	2.6	4.1	negative	238
Compound 9	2.9	3.7	negative	223
Compound 10	2.1	3.8	negative	n.d.

n.d.: not determined

^a Caco-2 permeability data was determined during routine compound characterization

Supplemental Material to DMD/2020/090563

Concentration dependency of the unbound partition coefficient $K_{p_{uu}}$ and its application to correct for exposure related discrepancies between biochemical and cellular potency of KAT6A inhibitors
Trünkle C., Lechner C., Korr D., Bouché L., Barak N., Fernández-Montalván A., Süssmuth R.D. and Reichel A.

Drug Metabolism and Disposition

Supplemental Table 2: Relevance of cellular saturation effects that occur at the unbound $IC_{50,cell}$ for the prediction of intracellular KAT6A exposure.

Compound	Unbound	Unbound	Unbound $IC_{50,cell}$	Difference between		Prediction improvement using corresponding $K_{p_{uu,cyto}}$
	$IC_{50,cell}$	$K_{m,app}$ [μM]	~ Unbound	unsaturated and		
	[μM]		$K_{m,app}$	corresponding $K_{p_{uu,cyto}}$		
WM-8014	0.018	6.3 ± 0.4	no	-	-	-
WM-1119	0.019	4.7 ± 2.2	no	-	-	-
Compound 1	0.43	0.68 ± 0.16	yes	1.8-fold	1.9-fold	
Compound 2	0.33	0.42 ± 0.05	yes	5.2-fold	2.1-fold	
Compound 3	0.22	0.074 ± 0.003	yes	22-fold	3.0-fold	
Compound 4	1.6	4.6 ± 2.8	yes	1.5-fold	-	-
Compound 5	0.67	1.69 ± 0.23	yes	1.3-fold	-	-
Compound 6	0.046	3.2 ± 1.9	no	-	-	-
Compound 7	0.14	1.24 ± 0.04	no	-	-	-
Compound 8	0.090	0.69 ± 0.14	no	-	-	-
Compound 9	0.12	1.0 ± 0.3	no	-	-	-
Compound 10	0.083	4.2 ± 0.5	no	-	-	-

Supplemental Material to DMD/2020/090563

Concentration dependency of the unbound partition coefficient $K_{p_{uu}}$ and its application to correct for exposure related discrepancies between biochemical and cellular potency of KAT6A inhibitors
Trünkle C., Lechner C., Korr D., Bouché L., Barak N., Fernández-Montalván A., Süssmuth R.D. and Reichel A.
Drug Metabolism and Disposition

Supplemental Table 3: Analytical method parameters for compound quantification via LC-MS/MS.

Compound	MW [g/mol]	RT [min]	Ionization Method	Q ₁ [Da]	CE [eV]	Q ₃ [Da]
WM-8014	384.4	0.41	ESI +	384.9	23	213.0
WM-1119	389.4	0.37	ESI +	389.9	69	172.0
Compound 1	460.5	0.45	ESI -	459.0	-34	140.8
Compound 2	510.2	0.53	ESI -	508.6	-38	225.7
Compound 3	602.7	0.54	ESI -	600.5	-38	189.8
Compound 4	437.5	0.43	ESI +	437.9	29	216.9
Compound 5	455.9	0.46	ESI +	455.9	25	163.0
Compound 6	420.5	0.44	ESI +	421.0	29	204.0
Compound 7	443.5	0.38	ESI +	426.9	33	205.0
Compound 8	435.5	0.45	ESI -	434.1	-44	145.8
Compound 9	434.5	0.44	ESI -	433.1	-40	168.8
Compound 10	410.4	0.40	ESI -	409.0	-82	143.9
Internal Standard	337.8	0.35	ESI +	337.9	25	210.9
Internal Standard	337.8	0.35	ESI -	335.9	-22	208.8

MW: Molecular Weight; RT: Retention Time; CE: Collision Energy; Q₁: Parent analyte mass; Q₂: Daughter analyte mass